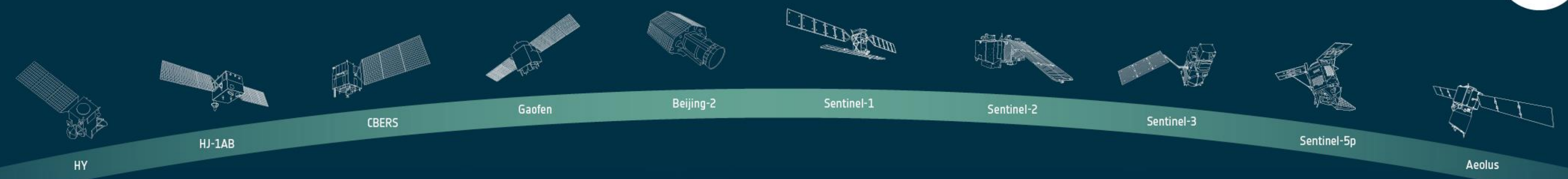

2022 DRAGON 5 SYMPOSIUM

MID-TERM RESULTS REPORTING

17-21 OCTOBER 2022

Synergistic Monitoring of Arctic Sea Ice from Multi-sensors

(ID: 57889)

Xi Zhang, Wolfgang Dierking, Li-jian Shi, Marko Mäkynen
Rasmus Tonboe, Juha Karvonen, Xiaoyi Shen, Meijie Liu

Outline

I. Introduction

II. Main results

III. Cooperation

IV. Young scientists and Publications

V. Next planning

I. Introduction

Objective

Upgrade and develop methodologies to retrieve quantitative sea ice information including measurements of thickness, drift, concentration, and detection of icebergs.

- Satellite data: Sentinel series, SMOS, CryoSAT-2, CFOSAT; HY-2, GF series
- Arctic and regional sites with seasonal ice cover

Dragon-2 5290	Dragon-3 10501	Dragon-4 32292，Part I	Dragon-5 57889
Only SAR Types	SAR + Optical Types, thickness, drift	Altimeter + SAR Thickness, deformation/drift	Multiple data More ice parameters

Team Composition

European Partners

- Dr. Wolfgang Dierking (PI) — University in Tromsø, Norway; Alfred Wegener Institute Helmholtz Center for Polar and Marine Research, Germany.
- Dr. Marko Mäkynen and Dr. Juha Karvonen — Finnish Meteorological Institute, Finland
- Dr. Rasmus Tonboe — Danish Meteorological Institute, Denmark

Chinese Partners

- Dr. Xi Zhang (PI) — First Institute of Oceanography, Ministry of Natural Resources
- Dr. Li-jian Shi, Tao Zeng and Qian Feng — National Satellite Ocean Application Service
- Dr. Jie Liu and Zhi Yuan — Institute of Spacecraft System Engineering, China Academy of Space Technology
- Dr. Xiaoyi Shen — Nanjing University
- Dr. Zhenyu Liu — South-Central Minzu University
- Dr. Meijie Liu — Qingdao University

II. Main Results

1. Sea ice concentration estimation with Chinese radiometer data
2. Sea ice chart and mapping with CFOSAT SWIM data
3. Sea ice thickness retrieval with active and passive microwave data
4. Sea ice thickness fusion with multi-platform altimeter data
5. Iceberg and melt pond detection with SAR and optical data

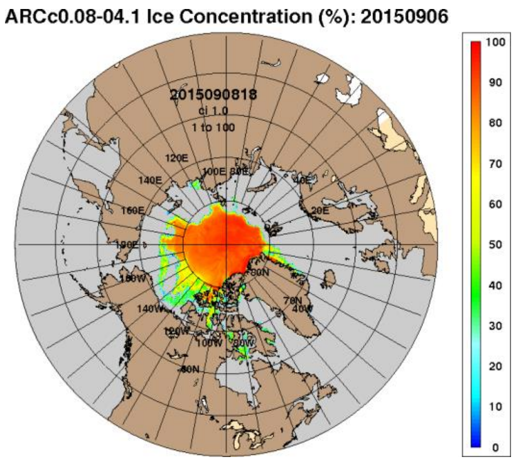

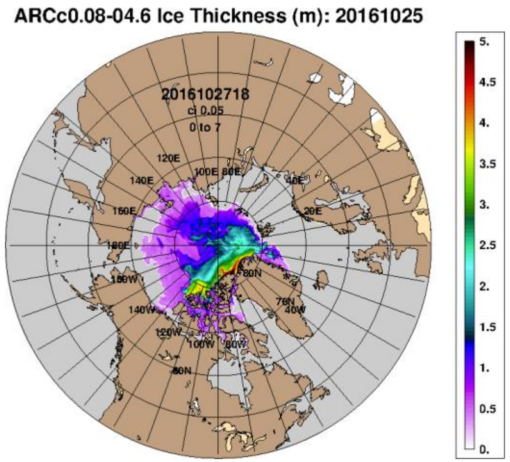

1. Sea ice concentration estimation with Chinese radiometer data

Contributors: NSOAS, FMI, and DMI

- Data source
  - HY-2B Scanning Microwave Radiometer (SMR)
  - FY-3C Microwave Radiation Imager (MWRI)
- Method
  - SIC was retrieved with intersensor calibration using the NASA Team (NT) algorithm.
  - Intersensor calibrations were performed between Tbs from DMSP/SSMIS and HY-2B/SMR or FY-3C/MWRI.

NT method included Dynamic Tie Points (DTPs)

- For MYI and FYI: mean Tb values for SIC > 95%.
- For ocean: mean Tb values for 0% SIC.

Weather filtering

- Atmospheric water vapor: GR(37/19) > 0.05 (NH) or 0.053 (SH)
- Cloud liquid water: GR(22/19)> 0.045

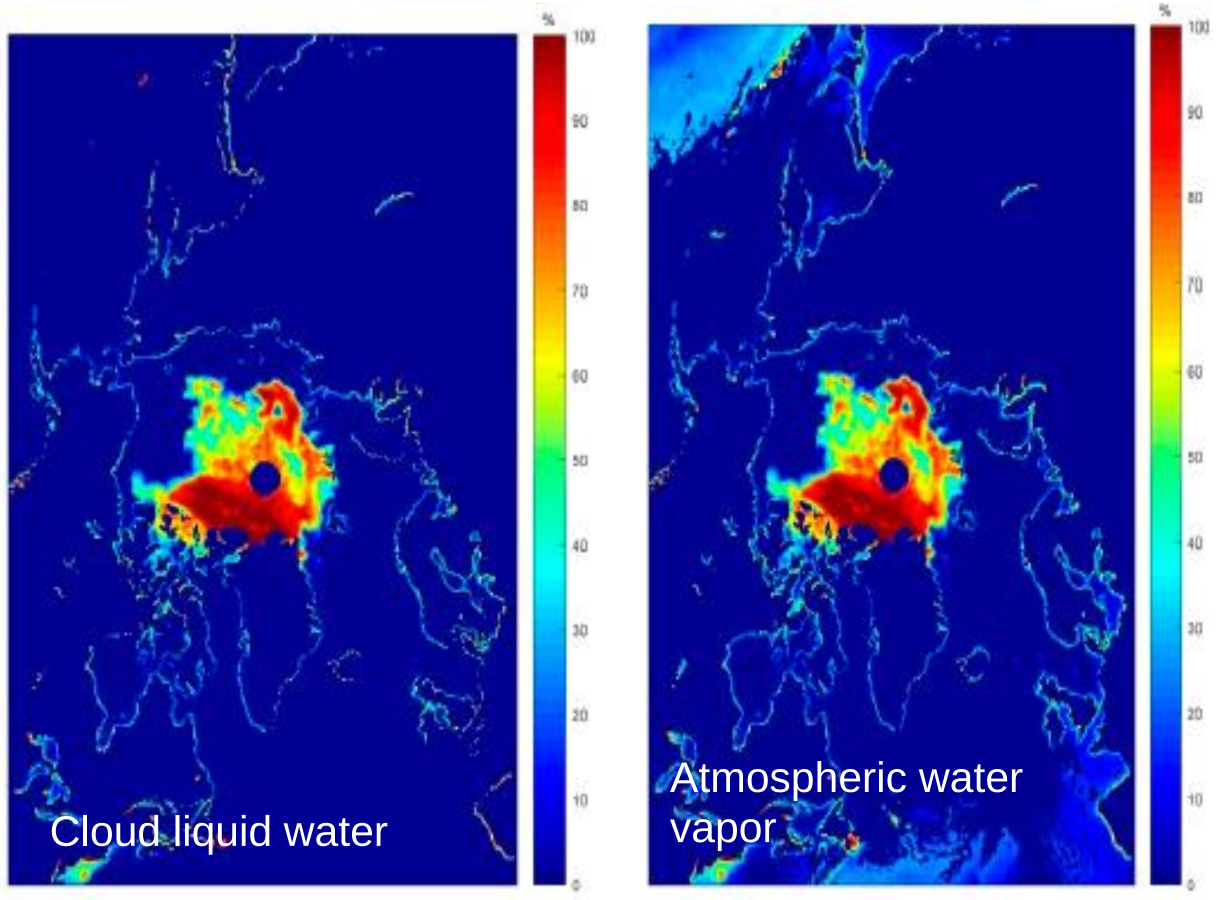

Land contamination effect removal

- Method described by Parkinson et al. (1987)

Validation

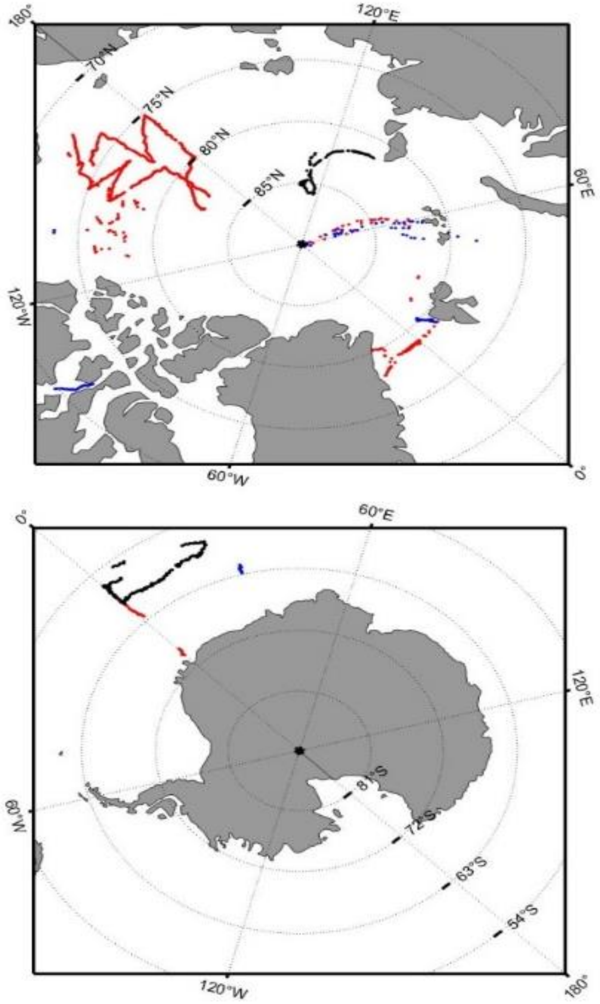

Ship SIC observation data
(2016, 2017, 2019)

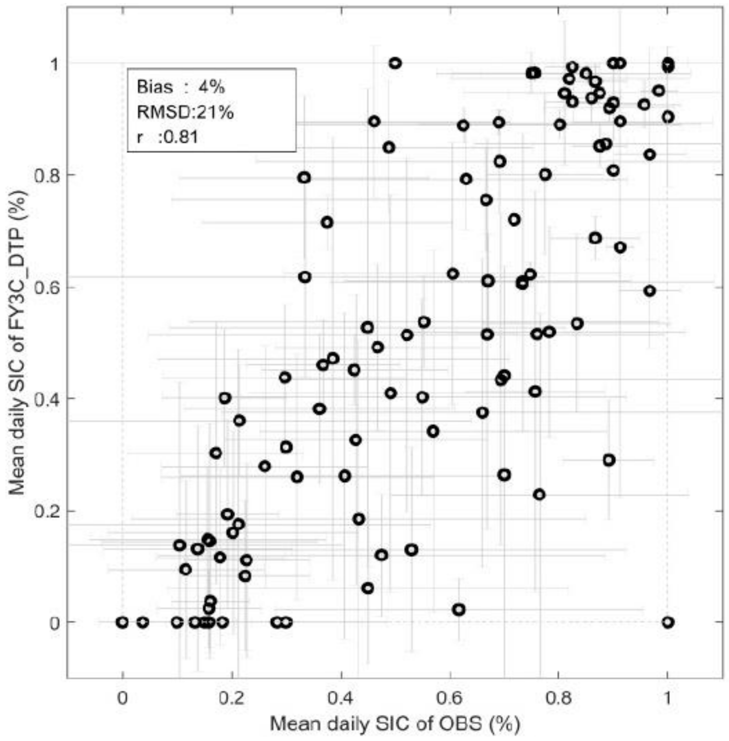

FY3C V.S OBS

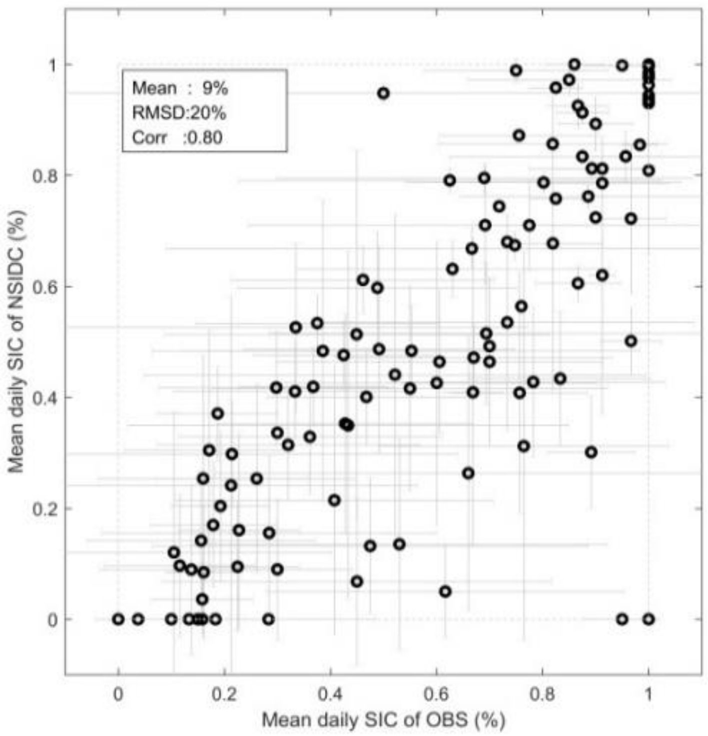

NSIDC V.S OBS

FY3C V.S. NSIDC: 0.53±1.50% for Antarctic

-0.27±1.85% for Arctic

2. Sea ice chart and mapping with CFOSAT/SWIM data

Contributors: FIO and QDU

- Data source
  - CFOSAT: Chinese-French Oceanic Satellite
  - SWIM: Surface Waves Investigation and Monitoring instrument

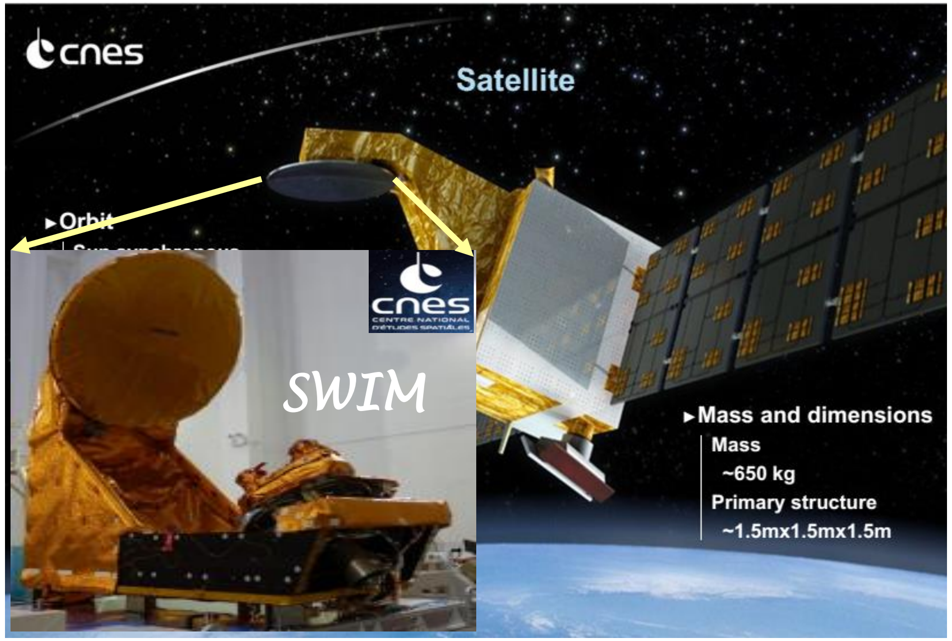

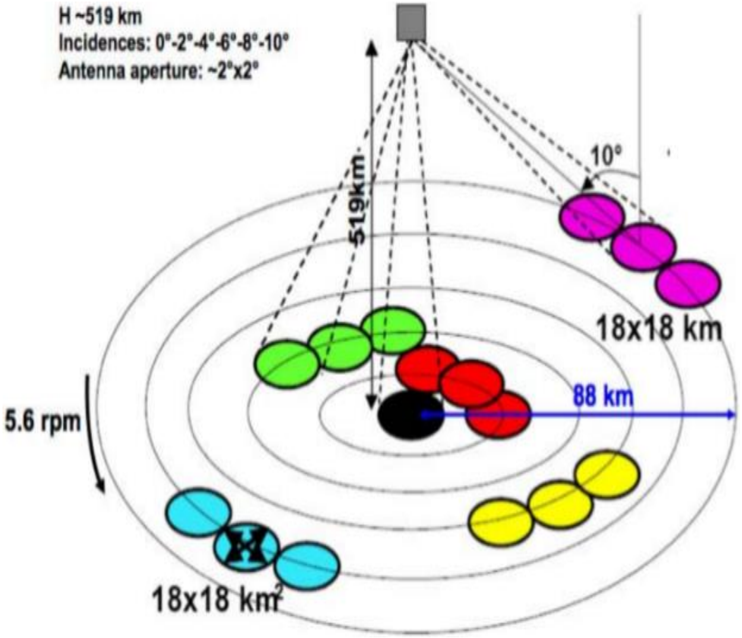

- Frequency: Ku (13.6 GHz)
- Incidence angle: 0/2/4/6/8/10º
- Azimuth angle: 0-360º

Auxiliary data

AARI

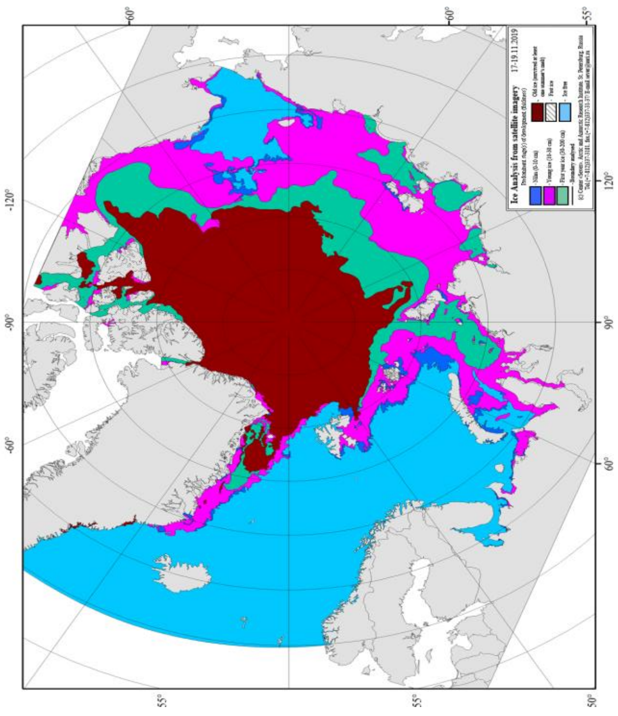

NSIDC

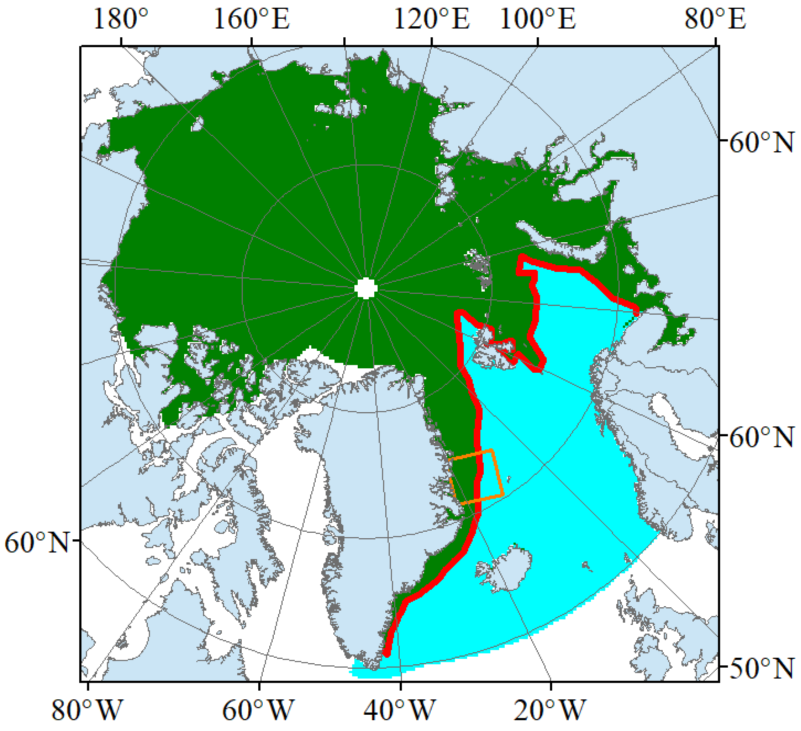

Sentinel-1

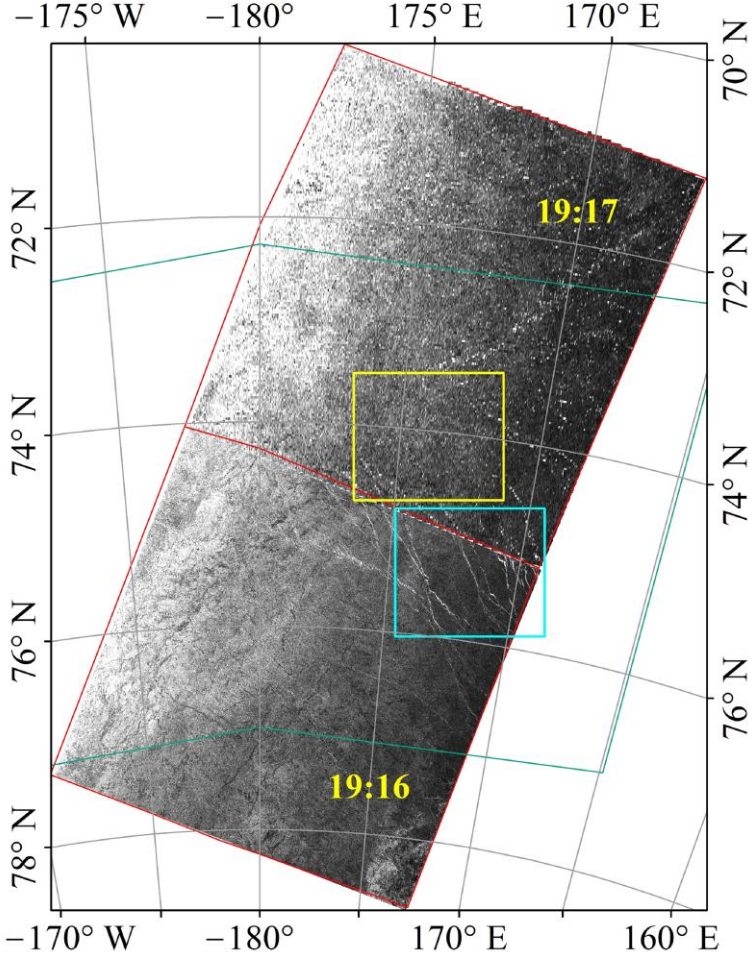

Thin ice	TI
First-year ice	FYI
Multi-year ice	MYI
Sea water	SW

Sea ice	FYI
Sea water	SW
Sea ice edge	SIE

Waveform features

1. Maximum power (MAX)
2. Backscattering power (BSP)
3. Pulse peakiness (PP)
4. Stack standard deviation (SSD)
5. Leading edge width (LEW)
6. Trailing edge width (TEW)

$$P_{max_\theta} = max(P_{i_\theta})$$

$$PP_\theta = \frac{P_{max_\theta}}{\sum_{i=1}^{n_\theta} P_{i_\theta}} \times n_\theta$$

$$SSD_\theta = \sqrt{\frac{\sum_{i=1}^{n_\theta}(P_{i_\theta} - \overline{P}_\theta)^2}{n_\theta}}$$

$$A_{1\theta} = P_{max_\theta} \cdot 0.95$$

$$A_{2\theta} = P_{max_\theta} \cdot 0.05$$

$$LEW = Bin(A_{1\theta}) - Bin(A_{2\theta})$$

$$TEW = Bin(A_{2\theta}) - Bin(A_{1\theta})$$

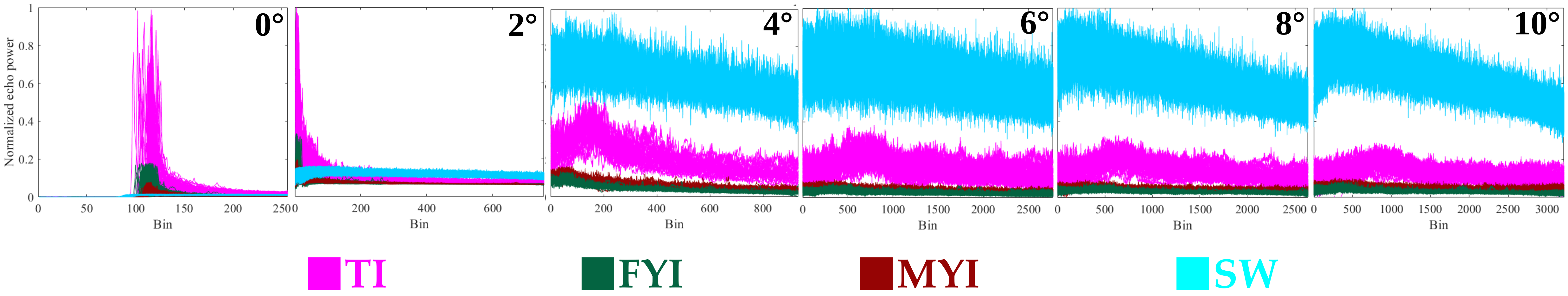

The characteristic of single feature and single angle

- Kolmogorov-Smirnov (K-S) distance

$$d_n = d_K(F_n, F_0) = \sup_x |F_n(x) - F_0(x)|$$

$$= \max_i \left(\max(F_0(x_{(i)}) - \frac{i-1}{n}, \frac{i}{n} - F_0(x_{(i)}) \right)$$

- Distinguish sea ice and sea water better than sea ice types
- Discrimination between FYI and MYI is the most difficult.
- Discrimination between TI and FYI is slightly better than that between TI and MYI.

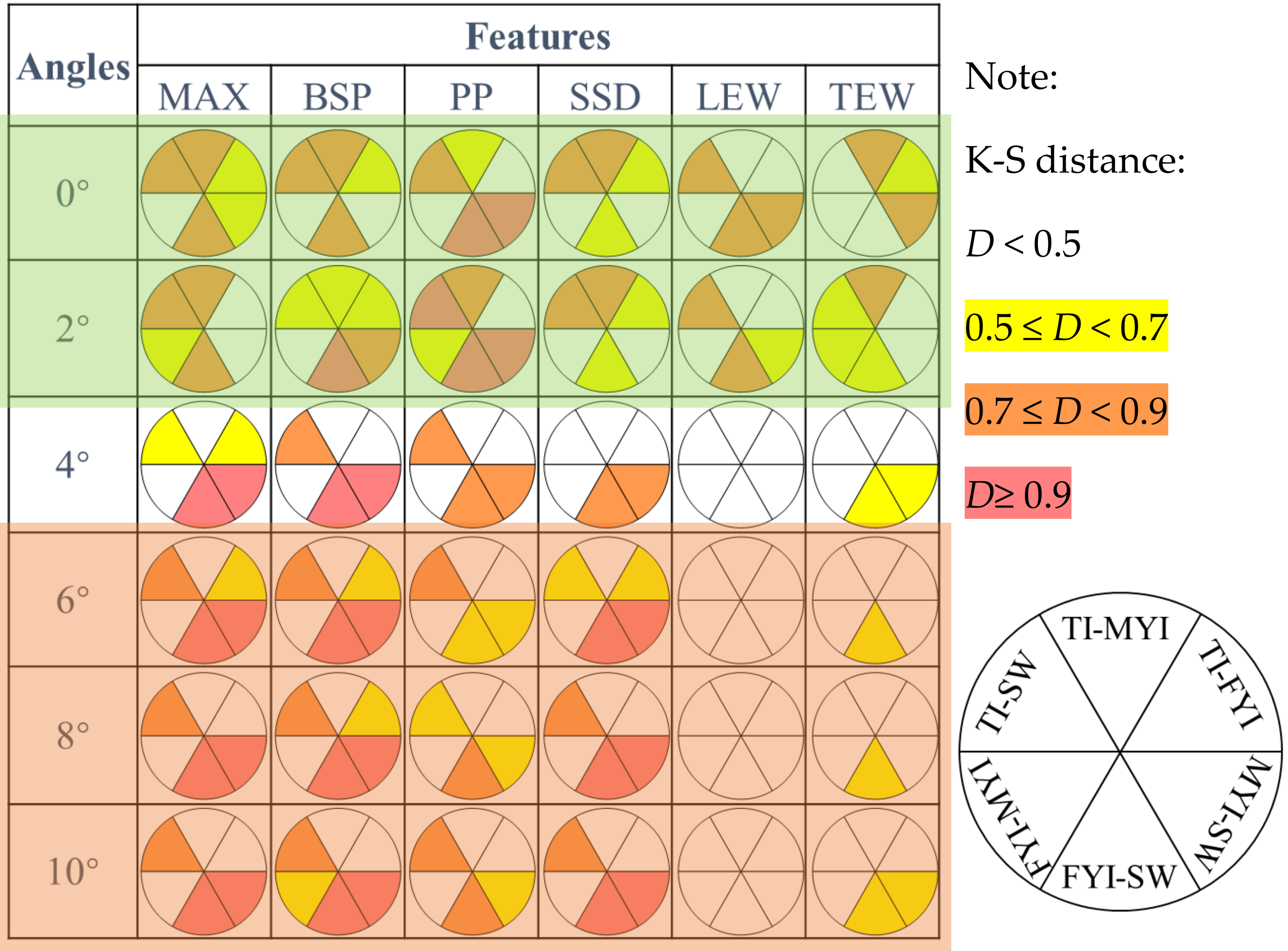

Sea ice type classification of multi-feature combinations using KNN method

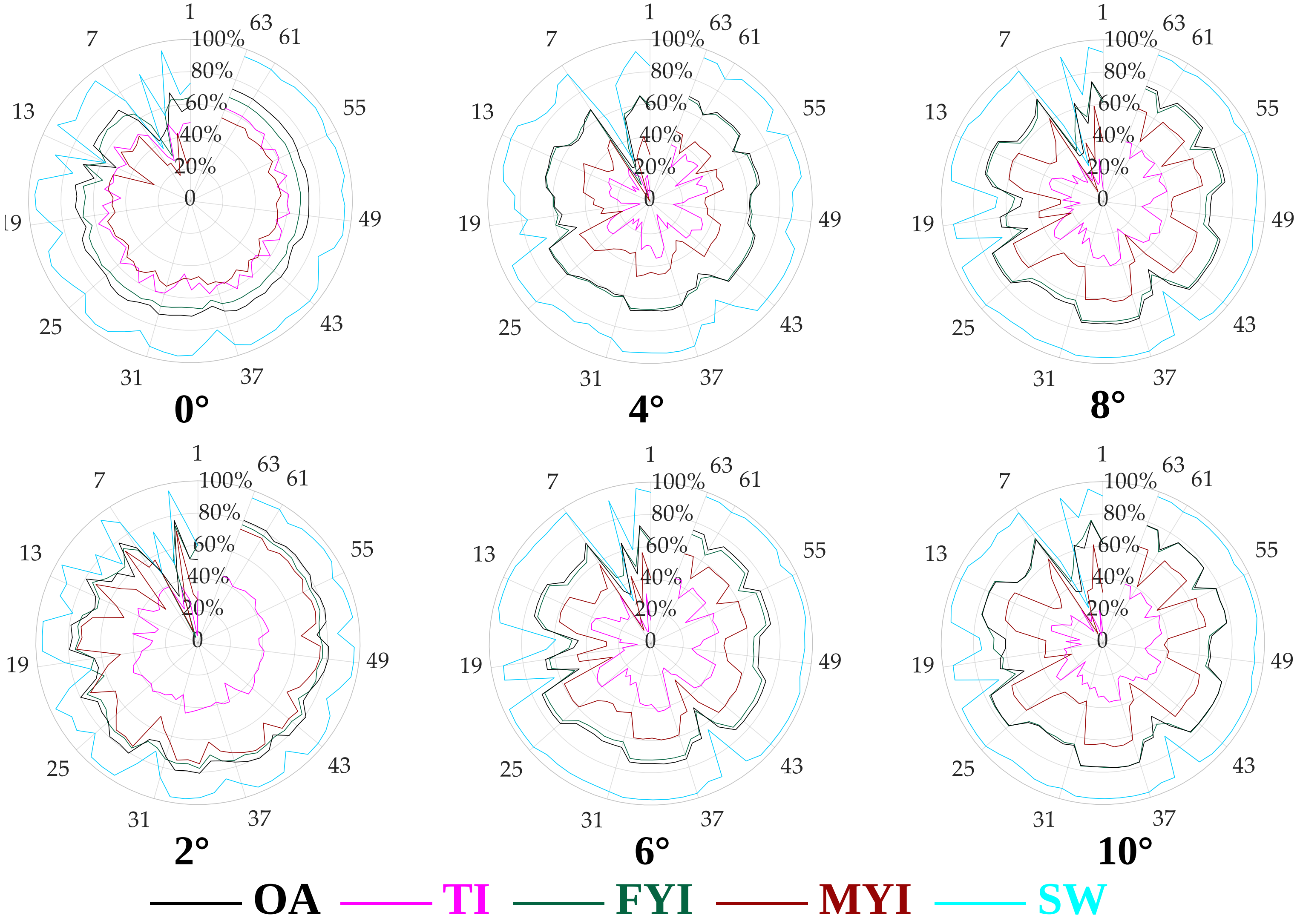

Angle	Overall Accuracy
0°	MAX-BSP-PP-SSD-LEW-TEW / 73.9%
2°	MAX-BSP-PP-SSD-TEW / 81.0%
4°	MAX-BSP-PP-SSD-TEW / 69.3%
6°	MAX-BSP-PP-SSD-LEW / 75.3%
8°	MAX-BSP-PP-SSD-LEW / 76.4%
10°	MAX-BSP-PP-SSD-TEW / 77.9%

Validation

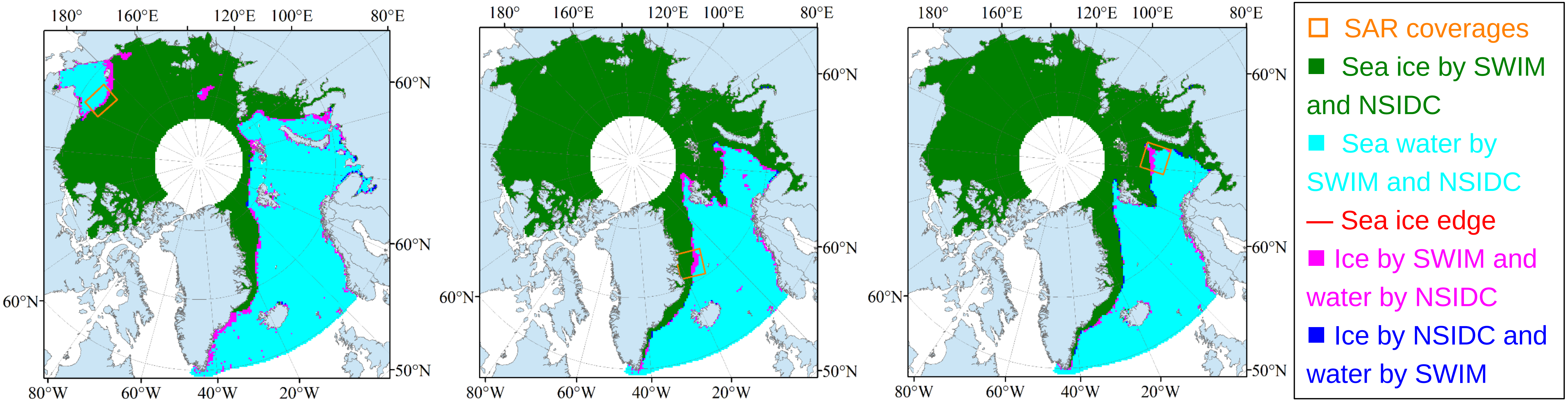

November 11th – 17th, 2020 | February 11th – 17th, 2021 | March 11th – 17th, 2021

The percentage of the grids with the same type:

- 94.8% (SR-7 from November 11th – 17th, and SAR/NR-1 on 11th)
- 97.7% (SR-7 from February 11th – 17th, and SAR/NR-1 on 17th)
- 98.2% (SR-7 from March 11th – 17th, and SAR/NR-1 on 17th)

NR-1: NSIDC results of 1 day

SAR-1: SAR results of 1 day

SR-7: SWIM results of 7 days

Sea ice edge

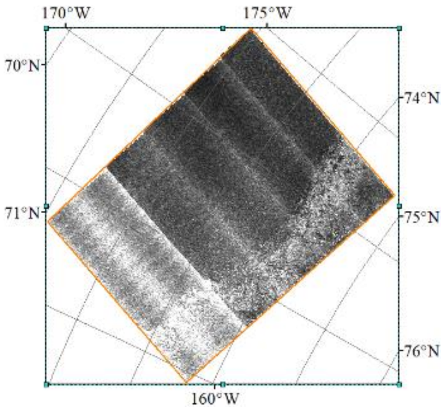

(A) Sentinel-1 SAR image, HV, at 18:04:46, Nov. 11th

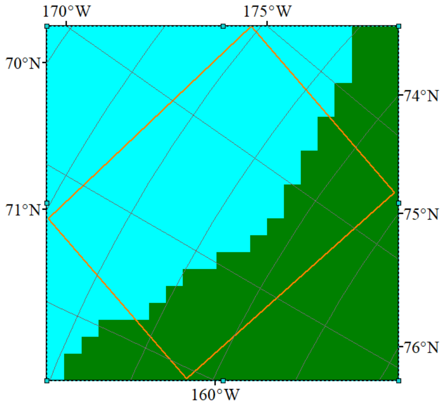

(B) Sea ice region of NSIDC on Nov. 11th

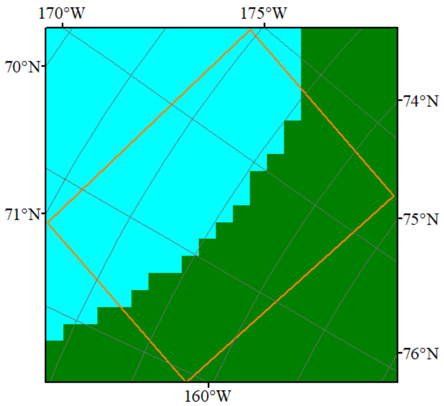

(C) Sea ice region of NSIDC on Nov. 14th

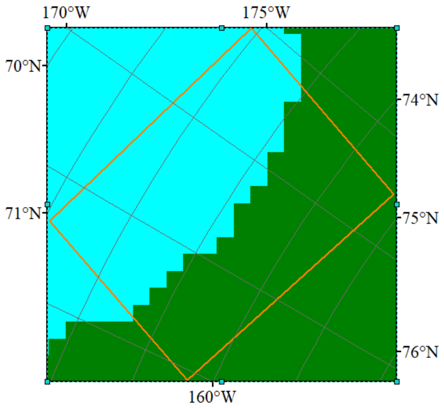

(D) Sea ice region of NSIDC on Nov. 17th

- SAR coverages
- Sea ice region
- Sea water region
- Ice edges of NR-1
- Ice edges of SR-1
- Ice edges of SR-7

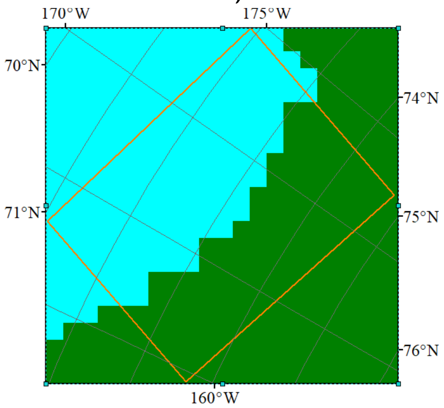

(E) Sea ice region of SWIM on Nov. 11th – 17th

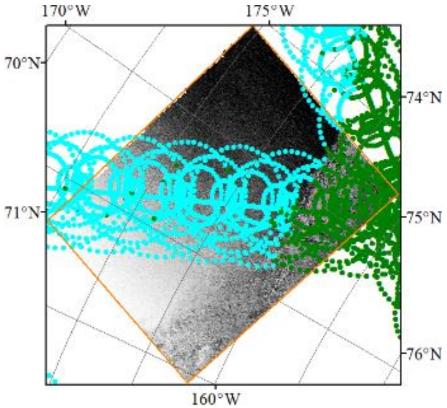

(F) Sentinel-1 image and SWIM data on Nov. 11th

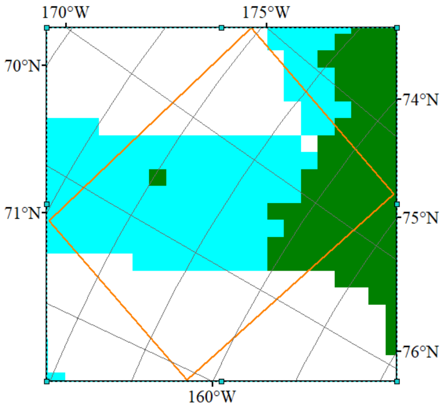

(G) Sea ice region of SWIM on Nov. 11th

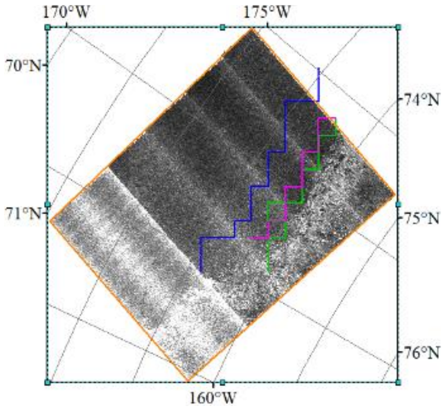

(H) Sea ice edge on Nov. 11th – 17th

SWIM can provide reliable daily sea ice edge (15% sea ice concentration).

3. Sea ice thickness retrieval with active and passive microwave data

Contributors: NSOAS and FMI

- Accurate determination of the snow cover over Arctic sea ice is significant for the retrieval of the sea ice thickness.
- Developed a new snow depth retrieval method over Arctic sea ice with a long short-term memory (LSTM) deep learning algorithm based on Operation IceBridge (OIB) snow depth data and brightness temperature data of AMSR-2.

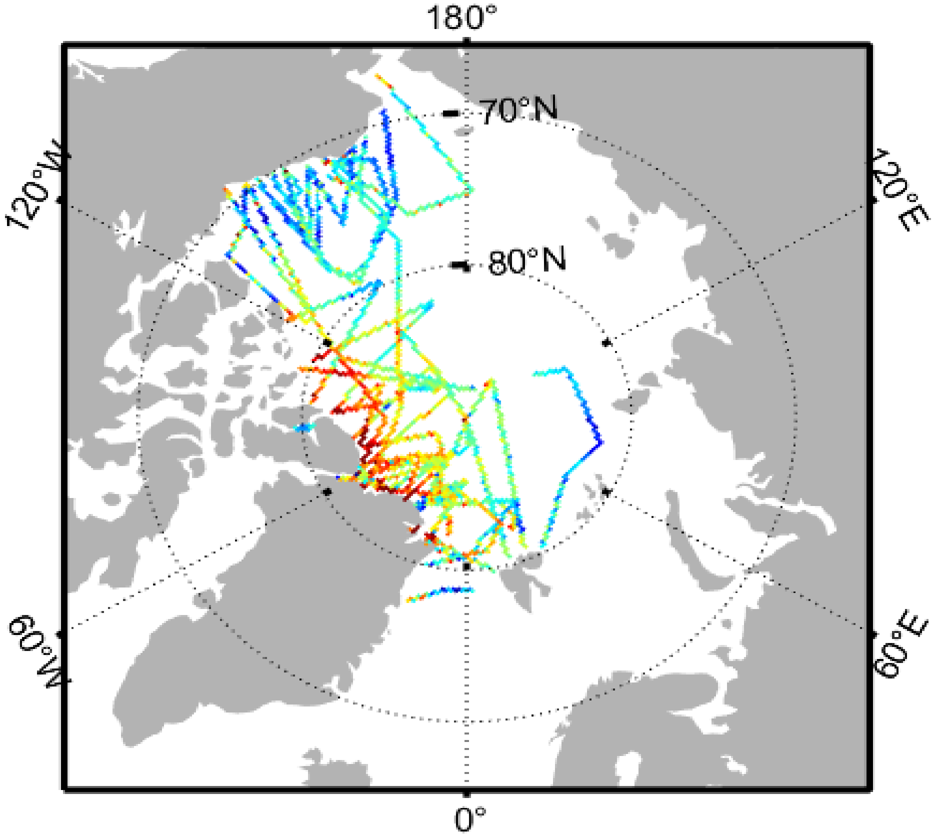

OIB data (2013-2019)

Method

- Brightness temperature correction

$$T_{b_{ice}}(f,p) = \frac{T_b(f,p) - (1 - SIC) * T_{bOW}(f,p)}{SIC}$$

- Input BT vector

$$GR(18.7/6.9) = \frac{T_{b_{ice}}(18.7V) - T_{b_{ice}}(6.9V)}{T_{b_{ice}}(18.7V) + T_{b_{ice}}(6.9V)}$$

$$GR(36.5/18.7) = \frac{T_{b_{ice}}(36.5V) - T_{b_{ice}}(18.7V)}{T_{b_{ice}}(36.5V) + T_{b_{ice}}(18.7V)}$$

$$PR(36.5) = \frac{T_{b_{ice}}(36.5V) - T_{b_{ice}}(36.5H)}{T_{b_{ice}}(36.5V) + T_{b_{ice}}(36.5H)}$$

- LSTM neural

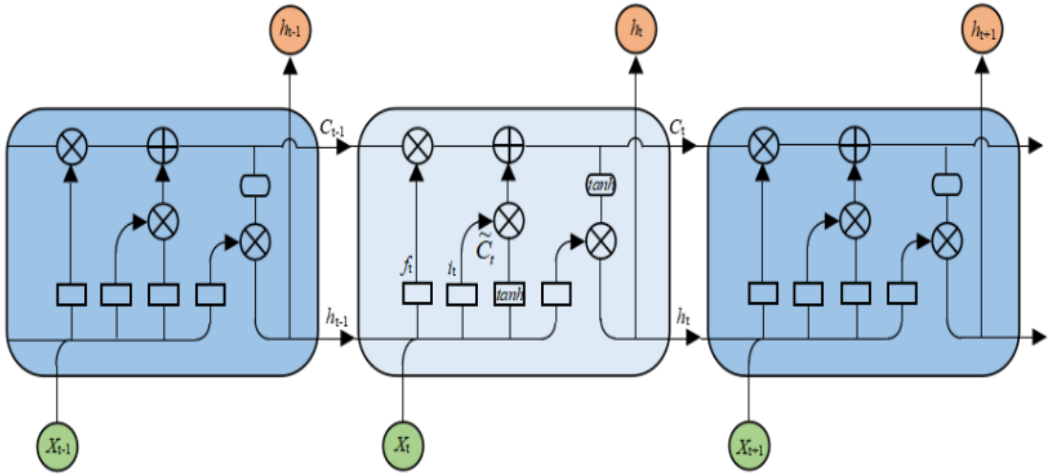

$$MAPE = \sum_{t=1}^{n} \left| \frac{sd_{OIB} - sd_{predicted}}{sd_{OIB}} \right| \times \frac{100\%}{n}$$

Validation

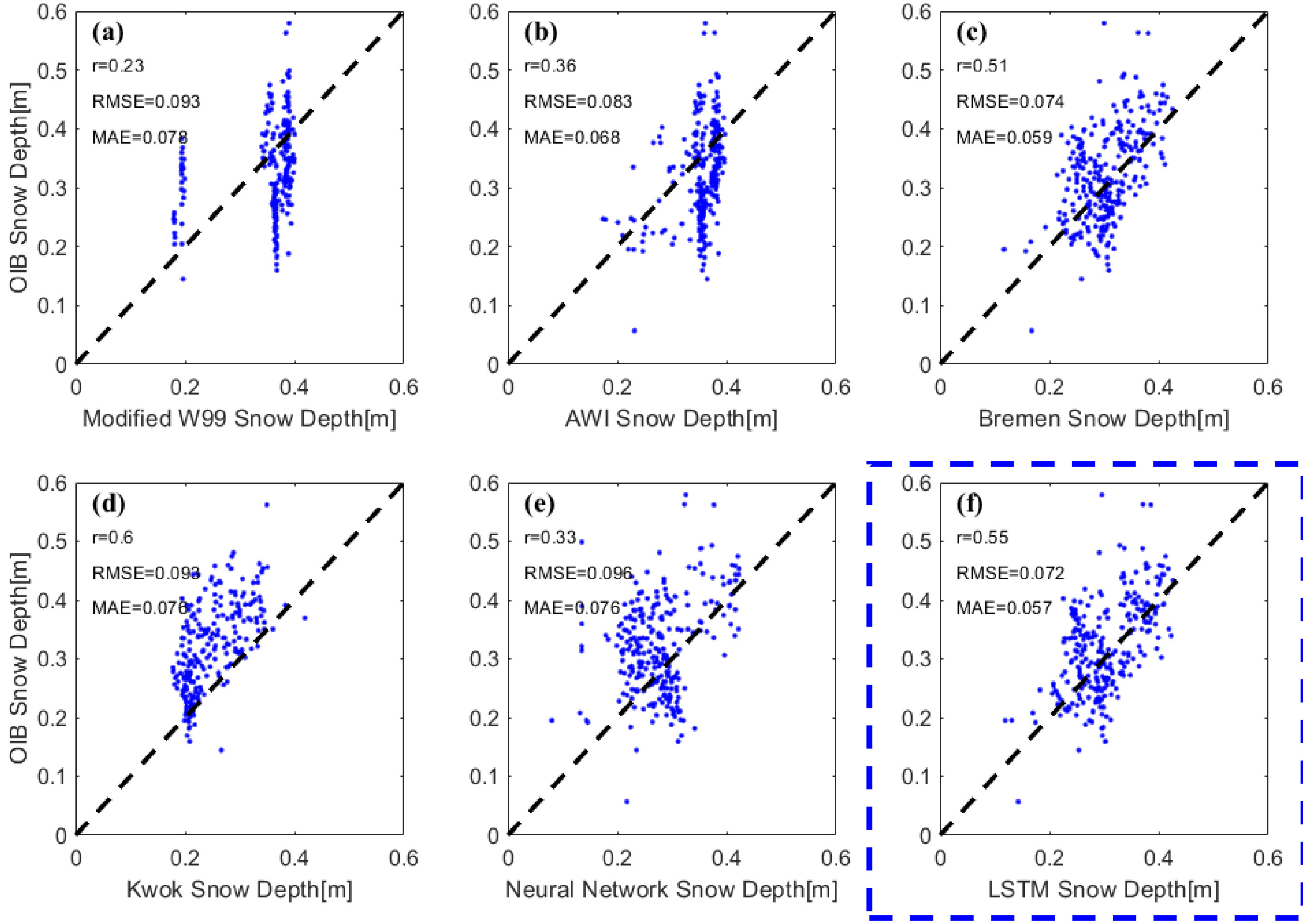

Compared with OIB snow depth data

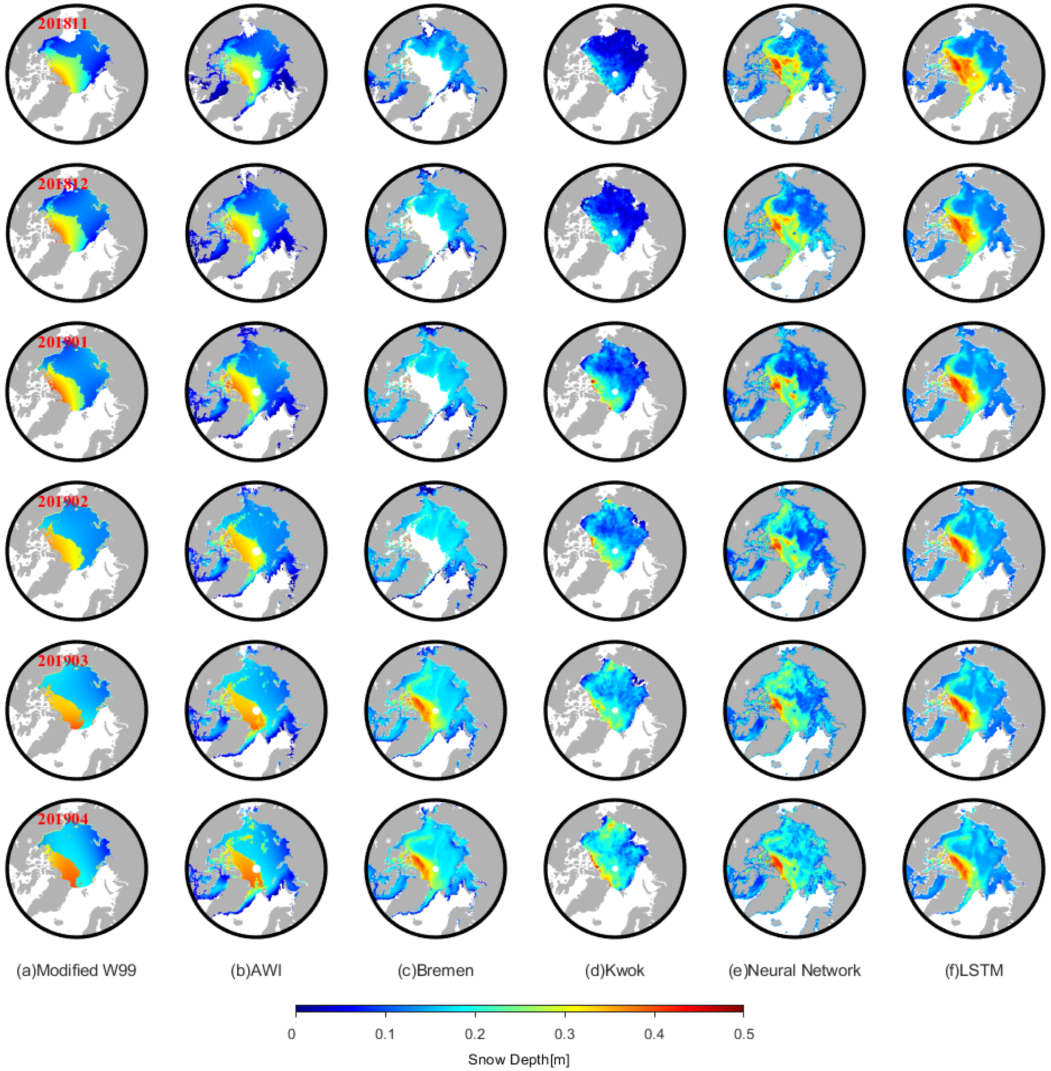

Snow depth derived from different methods

Sea ice thickness retrieval

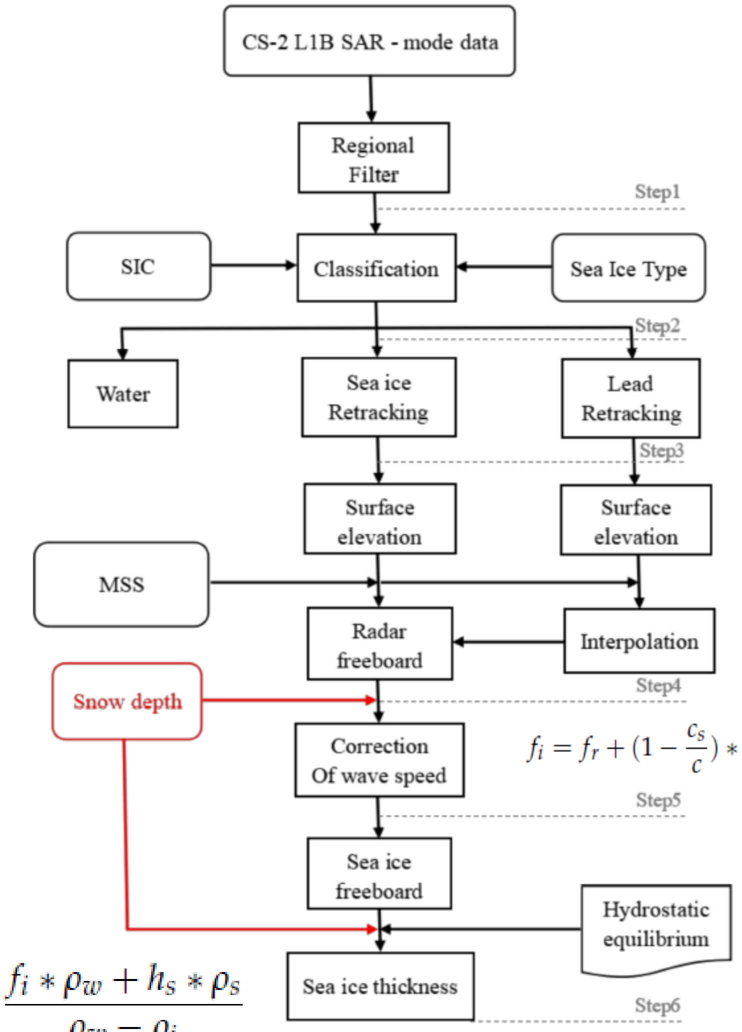

$$f_i = f_r + (1 - \frac{c_s}{c}) * h_s$$

$$T = \frac{f_i * \rho_w + h_s * \rho_s}{\rho_w - \rho_i}$$

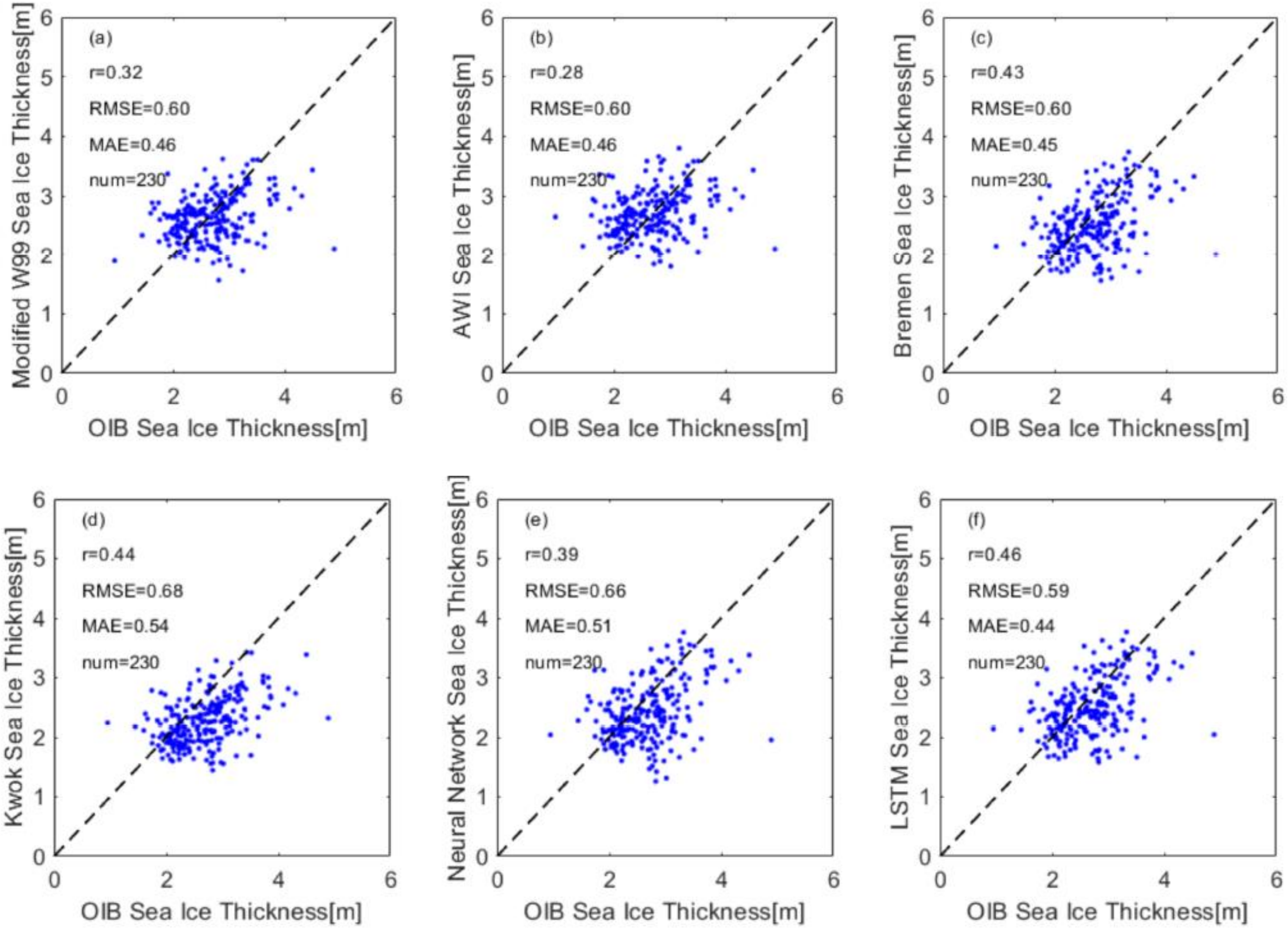

4. Sea ice thickness fusion with multi-platform altimeter data

Contributors: FIO and AWI

- Single satellite: low temporal resolution or large gaps between profiles.
- Fusion of data: CryoSat-2+Sentinel-3A+HY-2B to enhance temporal resolution and increase coverage.
- Data consistency: between satellite and field observations; inter-sensor.

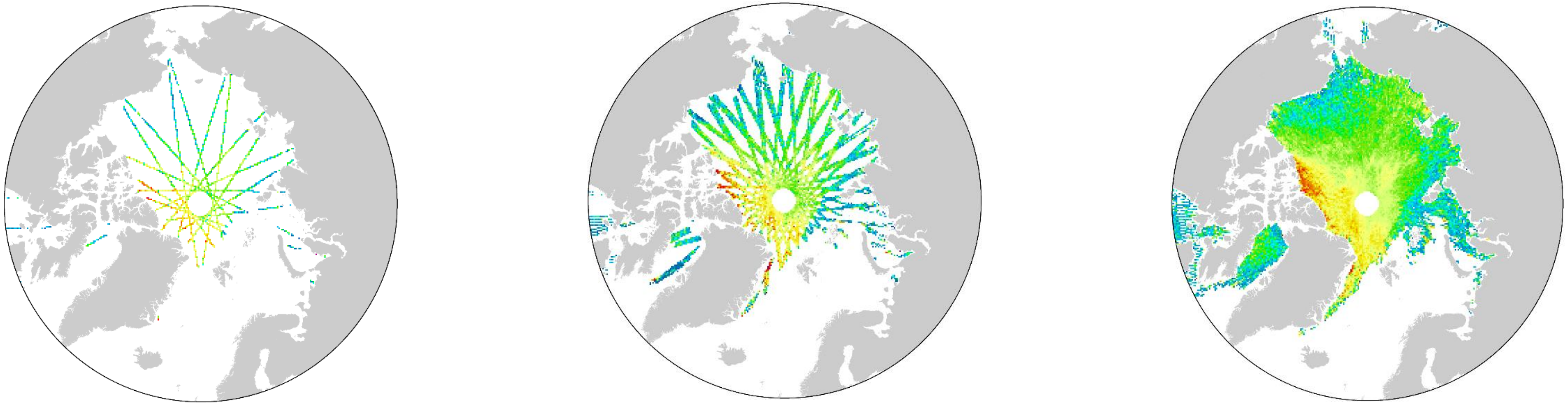

Daily Weekly Monthly

Ice freeboard consistency between CryoSat-2/Sentinel-3A and OIB

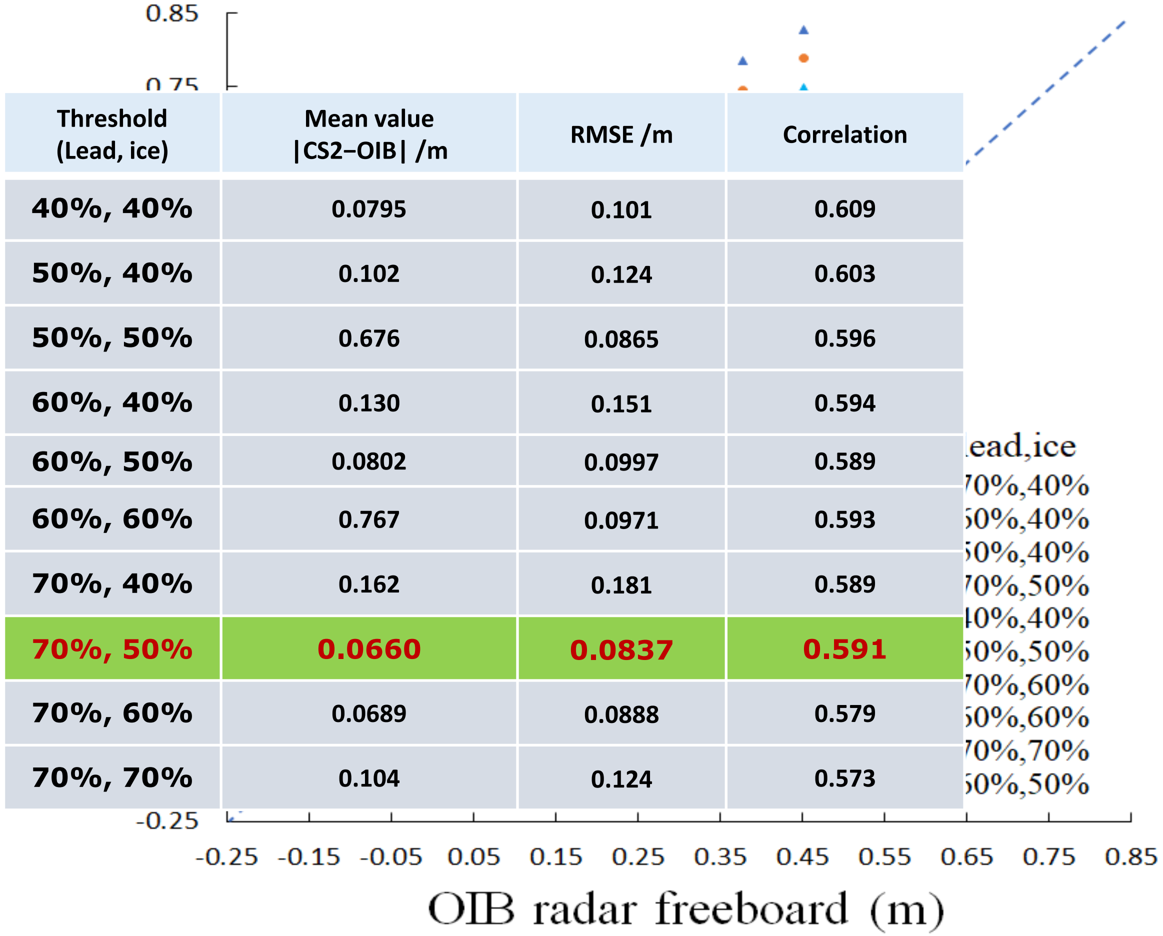

Threshold (Lead, ice)	Mean value |CS2–OIB| /m	RMSE /m	Correlation
40%, 40%	0.0795	0.101	0.609
50%, 40%	0.102	0.124	0.603
50%, 50%	0.676	0.0865	0.596
60%, 40%	0.130	0.151	0.594
60%, 50%	0.0802	0.0997	0.589
60%, 60%	0.767	0.0971	0.593
70%, 40%	0.162	0.181	0.589
70%, 50%	**0.0660**	**0.0837**	**0.591**
70%, 60%	0.0689	0.0888	0.579
70%, 70%	0.104	0.124	0.573

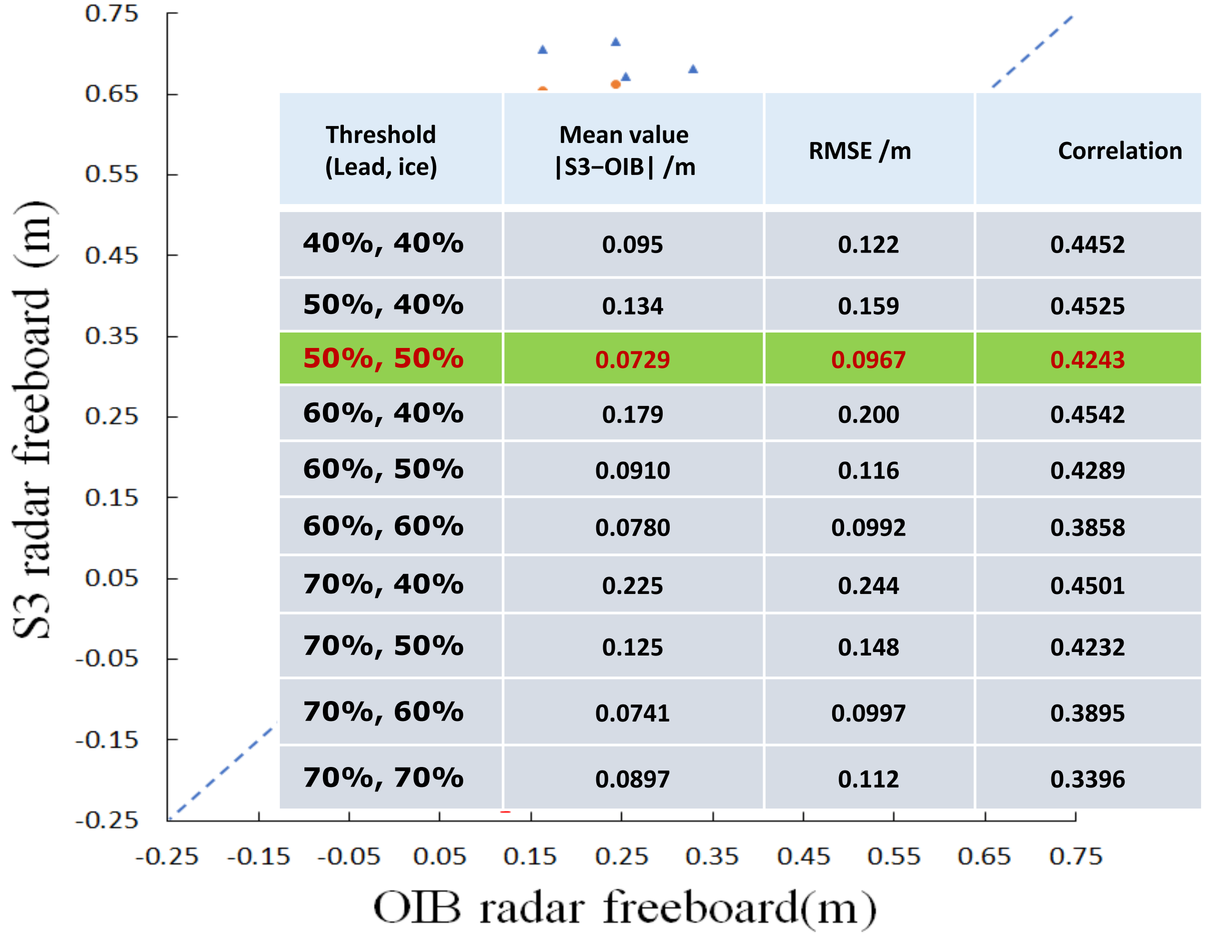

Threshold (Lead, ice)	Mean value |S3–OIB| /m	RMSE /m	Correlation
40%, 40%	0.095	0.122	0.4452
50%, 40%	0.134	0.159	0.4525
50%, 50%	0.0729	0.0967	0.4243
60%, 40%	0.179	0.200	0.4542
60%, 50%	0.0910	0.116	0.4289
60%, 60%	0.0780	0.0992	0.3858
70%, 40%	0.225	0.244	0.4501
70%, 50%	0.125	0.148	0.4232
70%, 60%	0.0741	0.0997	0.3895
70%, 70%	0.0897	0.112	0.3396

Ice thickness retrieval and multi-platform fusion

- Single satellite: conversion of freeboard into thickness assuming hydrostatic equilibrium.
- Multi-platform fusion method: areal weighting interpolation and inverse distance weighted averaging.
- The time resolution was increased from 1 month to half a month; for some areas up to 10 days.

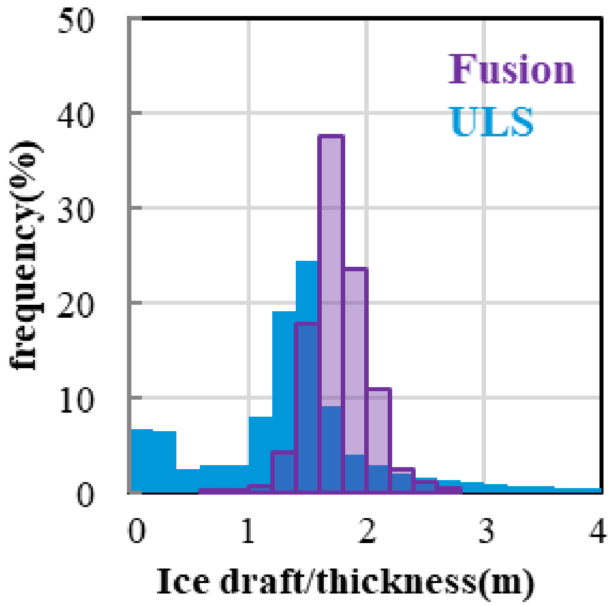

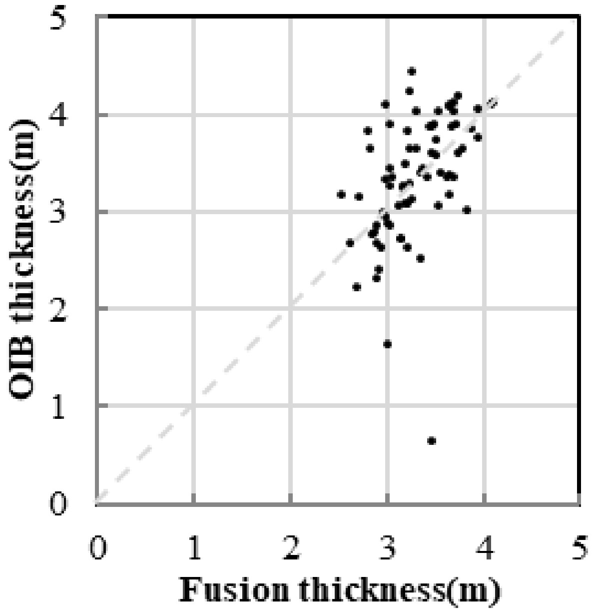

Satellite V.S. OIB

Apr 2018	MAE (m)	RMSE (m)	Correlation coefficient
Fusion	**0.44**	**0.60**	**0.62**
CS2	0.50	0.69	0.52
S3	0.59	0.84	0.39
Apr 2019	**MAE (m)**	**RMSE (m)**	**Correlation coefficient**
Fusion	**0.20**	**0.57**	**0.52**
CS2	0.50	0.69	0.36
IS2	0.88	1.06	0.34

5. Iceberg and melt pond detection with SAR and optical data

Contributors: AWI, SCMU, FIO, and NJU

- Improvement of iceberg detection in SAR images for operations and science, using multi-frequency data.
- AWI/UiT: Comparison of CFAR algorithms for iceberg detection
  - CFAR filters are tested and compared in Arctic regions.
  - Data: Sentinel-1 EW offers good coverage of the Arctic.

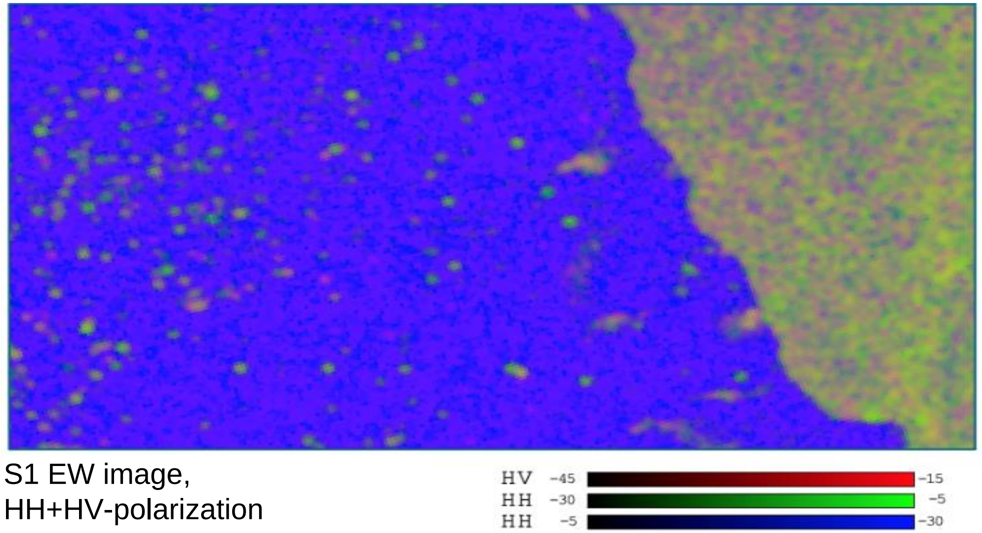

S1 EW image, HH+HV-polarization

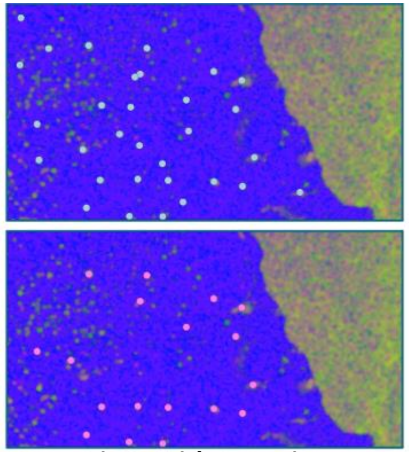

Detections with Gaussian CFAR filters using product (blue), and sum (purple) of the HV/HH bands

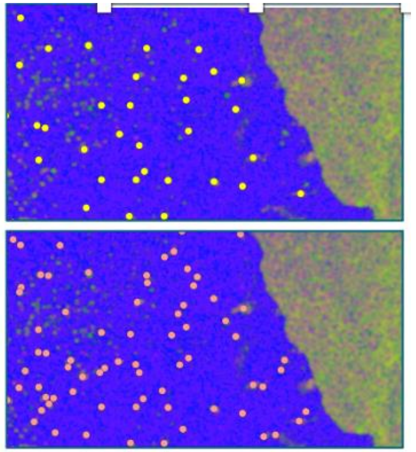

Objects detected with iterative (yellow), and Wishart-based (violet) CFAR filters

SCMU: Iceberg detection based on convolution neural network

- Data source: Radarsat-2 HV
- Method: adding an attention layer in U-net to enhance the training ability of neural networks.

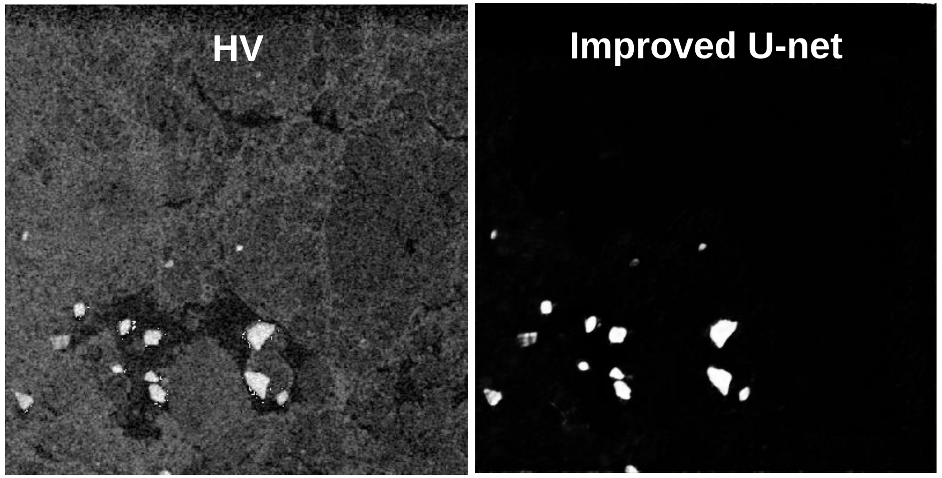

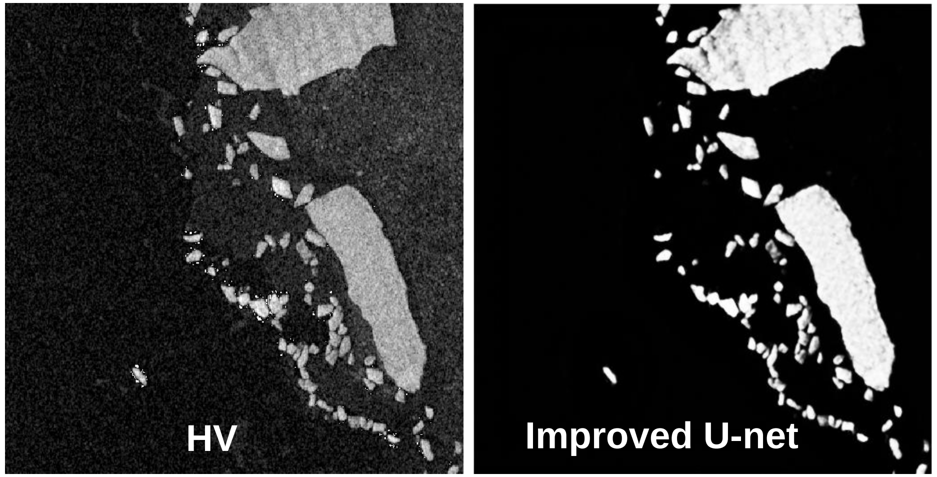

- A total of 1634 icebergs were manually marked;
- 1412 icebergs were identified by improved u-net, and the accuracy is 86.4%.

FIO: Iceberg Detection by L band Compact Polarimetric SAR

- Data source: ALOS PALSAR quad-pol converts to compact-pol.
- λ_2 represents the volume scattering, which has the largest contrast between iceberg and background.
- λ_2 is beneficial to the detection of iceberg.

$$C_{cp} = 2\left\langle \vec{k}_{cp}\vec{k}_{cp}^{*} \right\rangle = U_2 \begin{bmatrix} \lambda_1 & 0 \\ 0 & \lambda_2 \end{bmatrix} U_2^{-1}$$

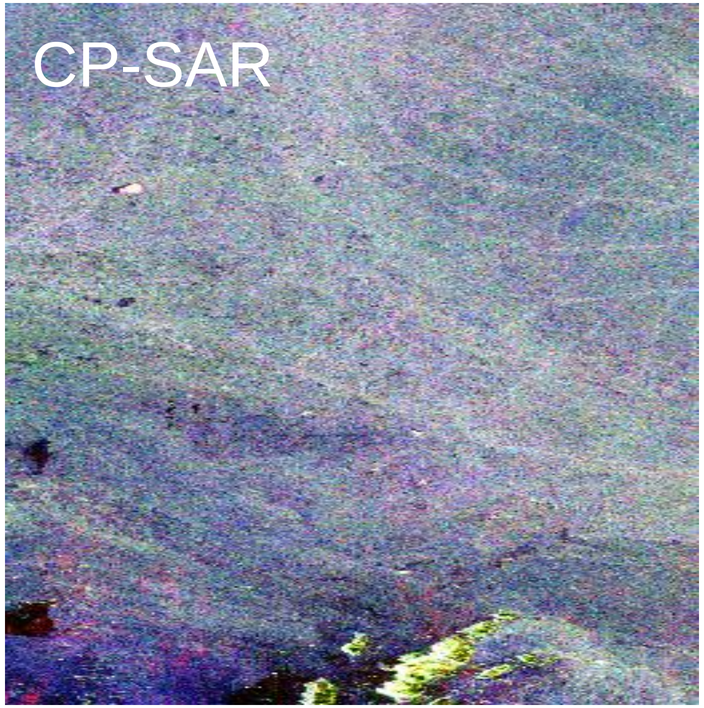

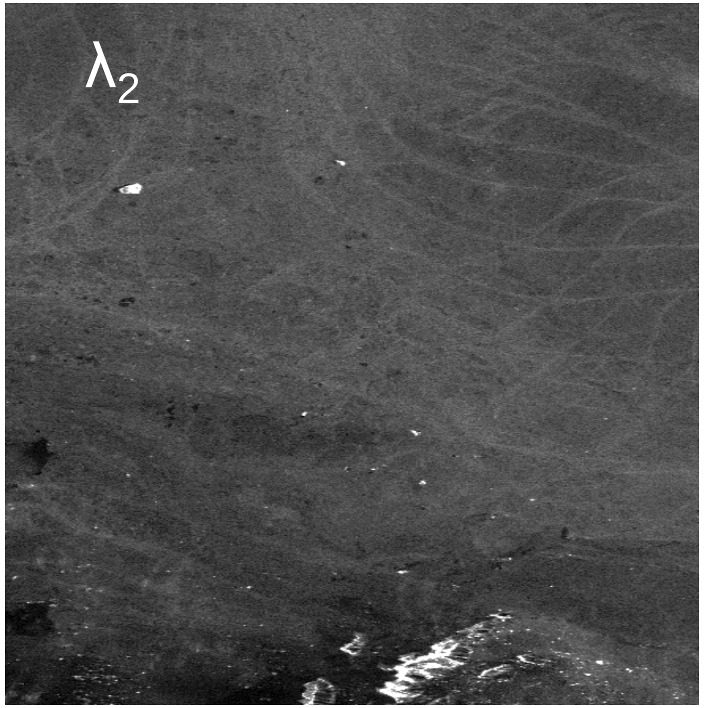

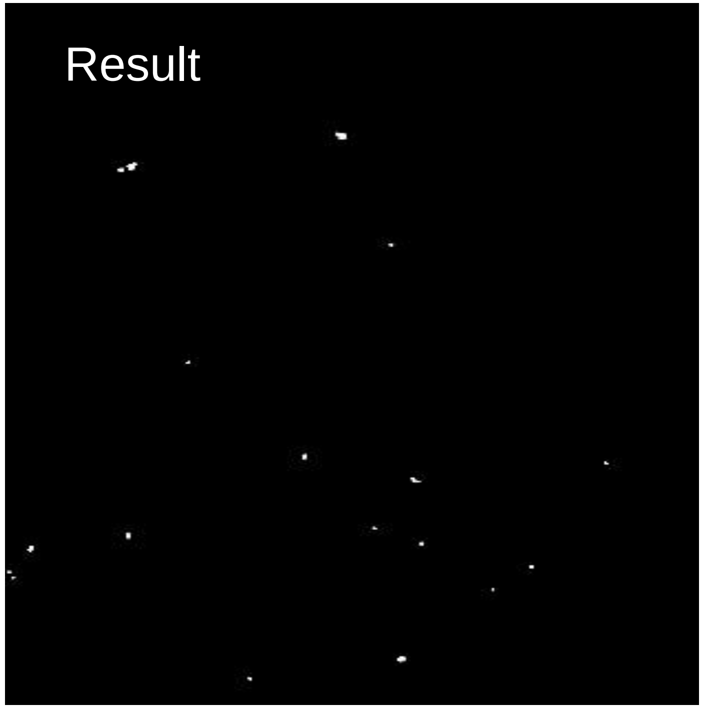

NJU: Melt pond Identification on sea ice with Sentinel-2 data

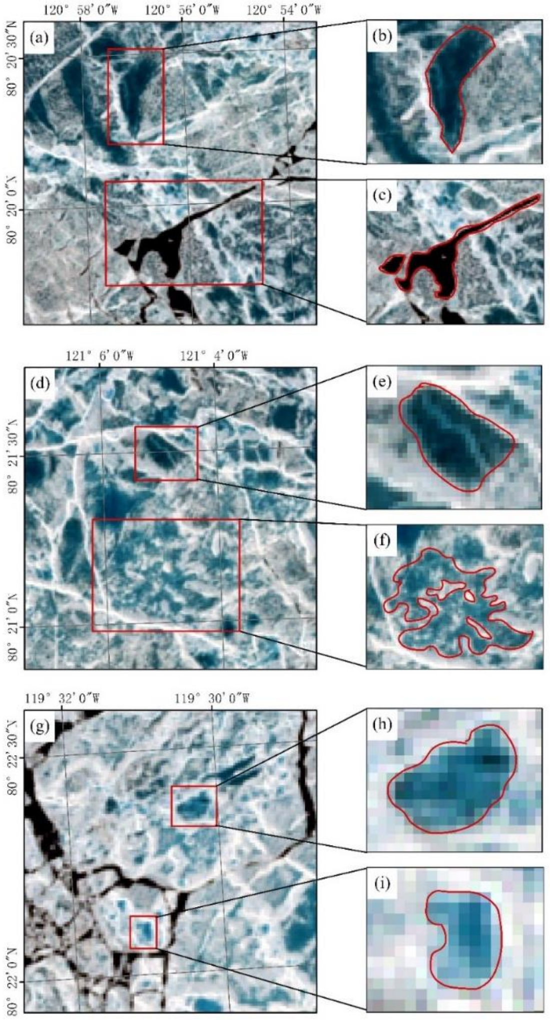

Samples of melt pond

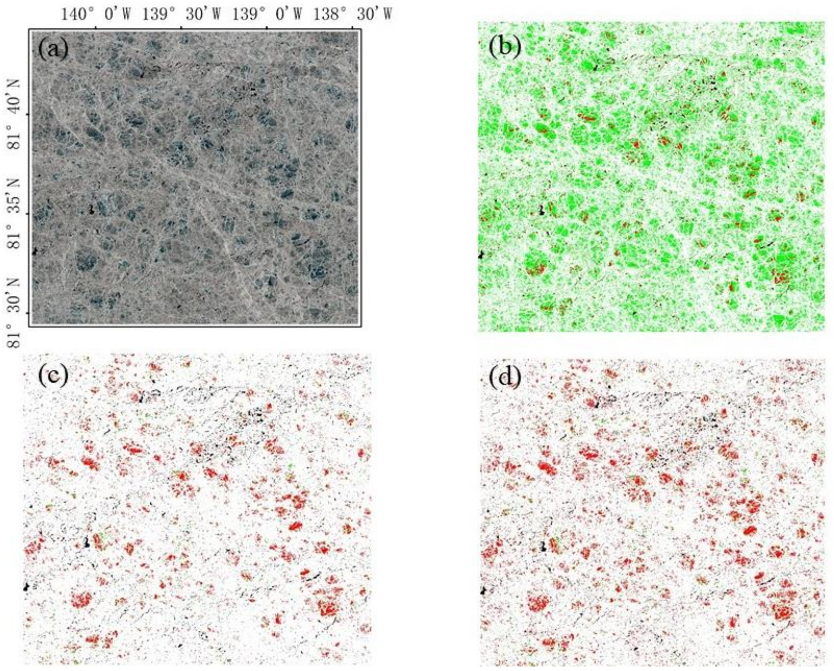

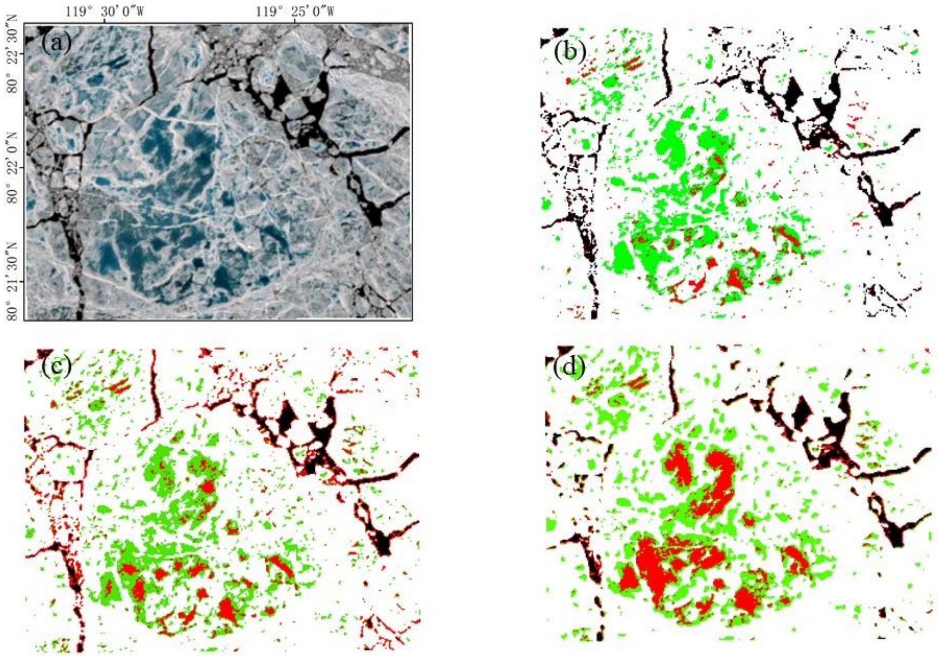

dark melt pond bright melt pond open water sea ice

(a) Sentinel-2 in 2020-7-8, (b) one-layer neural network , (c) Random Forest, (d) proposed method

(a) Sentinel-2 in 2020-6-30 , (b) one-layer neural network , (c) Random Forest, (d) proposed method

light melt pond: 87.4%

dark melt ponds: 75.2%

EO Data Delivery

Data access (list all missions and issues if any). NB. in the tables please insert cumulative figures (since July 2020) for no. of scenes of high bit rate data (e.g. S1 100 scenes). If data delivery is low bit rate by ftp, insert "ftp"

ESA Third Party Missions	No. Scenes
1. ALOS PALSAR	6
2. RadarSAT-2	12
3.	
4.	
5.	
6.	
Total:	
Issues: Iceberg detection, University in Tromsø/Norway: ESA-Agreement with JAXA: PALSAR-2 FB and WB images since April 2019 (not specifically via Dragon)	

ESA Third Party Missions	No. Scenes
1. Sentinel-1	45
2. Sentinel-3 SLAT	2017~2021
3. CryoSat-2	2017~2021
4.	
5.	
6.	
Total:	
Issues: Iceberg detection, University in Tromsø/Norway: S1 and S2 images via Science Hub since April 2019 (not specifically via Dragon)	

Chinese EO data	No. Scenes
1. HY-2B	2018~2021
2. GF-3	23
3. FY-3C	2019~2021
4.	
5.	
6.	
Total:	
Issues:	

III. Cooperation

- FIO, AWI, FMI, and NSOAS continue to develop sea ice thickness retrieval algorithms.
- NSOAS, FMI and DMI develop sea ice concentration estimation and SIC noise reduction algorithms.
- Joint effort by AWI/UiT, FIO, FMI, and SCMU is in preparation to deal with the detection of icebergs in sea ice.
- Cooperations with ice services world-wide (e.g. Denmark, Norway, Sweden, Canada, US, Argentina), plus Chalmers Technical University in Gothenburg, Sweden.
- The work of sea ice thickness detection work was selected for China-EU Space Science and Technology Cooperation Briefing.
- We were invited to introduce our work in webcasts.


中欧空间科技合作
简讯

2021 年第 1 期(总第 1 期)

科技部国家遥感中心 2021 年 4 月 1 日

“龙计划”项目：高时间分辨率的海冰厚度融合探测产品 单一高度计只能得到以月为分辨率的网格化海冰厚度产品，时间分辨率低，难以满足业务预报需求。为此，项目组综合 CryoSat-2、Sentinel-3 和 HY-2 数据，发展了多卫星高度计的海冰厚度融合探测方法，将海冰厚度网格化产品的时间分辨率从 1 个月提高至半个月，且空间分辨率保持不变，该产品为极地预报提供更高时间分辨率的初始场。

IV. Young scientists and Publications

- At present, Chinese students are the main participants in the project.
- A proposal was submitted to support Training of Young European Scientist from University in Tromsø (PhD level) working on iceberg detection.

① Shi L., et al., Sea Ice Concentration Products over Polar Regions with Chinese FY3C/MWRI Data. Remote Sens. 2021, 13, 2174.

② Dierking W. and Zhang X. are co-authors, “Using New Ocean Remote Sensing Data for Operational Applications: Results from the Dragon 4 Cooperation Project”, Remote Sensing, 2021, 13, 2847.

③ Dierking W. et al., “Synergistic used of L- and C-band SAR satellites for sea ice monitoring”, IGARSS 2021.

④ Zhang X. et al., “Arctic Sea Ice Classification Based on HY-2B Dual-band Radar Altimeter Data during Winter to Early Spring Conditions”, IEEE JSTARS, 2021, 14: 9855-9872.

⑤ Dong Z. et al., A Suitable Retrieval Algorithm of Arctic Snow Depths with AMSR-2 and Its Application to Sea Ice Thicknesses of Cryosat-2 Data. Remote Sensing, 2022, 14, 1041.

⑥ Liu M., et al. “Arctic Sea Ice Classification Based on CFOSAT SWIM Data at Multiple Small Incidence Angles.” Remote Sensing, 2021, 14, 91.

⑦ Liu M., et al. “Sea ice recognition for CFOSAT SWIM at multiple small incidence angles in the Arctic.” Front. Mar. Sci., 2022, 9: 986228.

⑧ Bao L., Zhang X., Cao C., et al. Impact of Polarization Basis on Wind and Wave Parameters Estimation Using the Azimuth Cutoff from GF-3 SAR Imagery. IEEE Transactions on Geoscience and Remote Sensing, 2022. https://doi.org/10.1109/TGRS.2022.3204409

⑨ Zhang R., Zhang J., Zhang X., et al. Influence of Radar Parameters and Sea State on Wind Wave-Induced Velocity in C-Band ATI SAR Ocean Surface Currents. Remote Sensing, 2022: 4135. https://doi.org/10.3390/rs14174135

⑩ Guan Y, Zhang J, Zhang X, et al. Study on the activity laws of fishing vessels in China's sea areas in winter and spring and the effects of the COVID-19 pandemic based on AIS data. Frontiers in Marine Science, 2022: 588. https://doi.org/10.3389/fmars

⑪ Cao C., Zhang J., Zhang X., et al. Modeling and Parameter Representation of Sea Clutter Amplitude at Different Grazing Angles. IEEE Journal on Miniaturization for Air and Space Systems. (Accepted)

⑫ Guan Y., Zhang J., Zhang X., et al. Impacts of the COVID-19 Epidemic on Ship Activity in Dongying Port Waters. IEEE Journal on Miniaturization for Air and Space Systems. (Accepted)

⑬ Fang H., Zhang X., et al. Evaluation of Arctic Sea Ice Drift Products based on FY-3, HY-2, AMSR2 and SSMIS Radiometer Data. Remote Sensing. (Accepted)

V. Next planning

- Iceberg detection: improvement of algorithms, comparison and selection of optimal one(s), collection of data for validation, validation, building semi-operational environment (the key work of Sino-European joint effort).
- Sea ice drift: develop algorithm for Chinese HY-2 radiometer and for alignment of C- and L-band images (at AWI and University in Tromsø)
- Sea ice thickness: Altimeter + SAR to improve the spatial resolution of sea ice thickness product.

Thanks for your attention!